Carbon 116 (2017) 391–397

Contents lists available at ScienceDirect

Carbon

journal homepage: www.elsevier.com/locate/carbon

# Enhanced stress wave attenuation of single-walled carbon nanotube lattice via mass mismatch-induced resonance

Bowen Zheng [a, b], Jun Xu [a, b, *]

[a] Department of Automotive Engineering, School of Transportation Science and Engineering, Beihang University, Beijing, 100191, China
[b] Advanced Vehicle Research Center (AVRC), Beihang University, Beijing, 100191, China

ARTICLE INFO

*Article history:*
Received 25 November 2016
Received in revised form
14 January 2017
Accepted 5 February 2017
Available online 9 February 2017

ABSTRACT

Nanoscale homogeneous single-walled carbon nanotube lattice exhibits extraordinary attenuation performance and ultrahigh specific energy absorption upon high-velocity impact. However, upon relatively low impact velocity (for example, < 1000 m/s), this system does not possess a good stress wave attenuation performance where severe damage may still occur. To overcome this disadvantage, a new attenuation mechanism is introduced to carbon nanotube lattice via the creation of mass mismatch, i.e. carbon nanotube dimer lattice. Under specific mass ratio, a strong inherent resonance happens, resulting in an evident attenuation of the propagating pulse. The joint effect of mass mismatch-induced resonance and dissipative nature of carbon nanotube lattice make it ideal for both high and low-velocity impacts. Additionally, specific energy absorption is improved due to the mass reduction. This work reveals the possibility to achieve much higher energy dissipation by exploiting the system's inherent dynamics, suggesting a new strategy of lightweight design of protective devices and the potential of technological applications of nanoscale nonlinear granular crystals.



## 1. Introduction

Phononic crystals and acoustic metamaterials, as artificially structured composite materials, have been generating great scientific interests in decades [1–5]. Dispersion characteristics of vibrational waves can be manipulated through Bragg scattering [2,3] or localized resonance [4], thereby providing a powerful approach to tailoring the flow of mechanical energy. In the nonlinear regime, granular crystals governed by Hertzian contact [6] exhibit novel dynamics such as solitary waves [7–10] and discrete breathers [11], having stimulated many exciting technological applications, e.g. acoustic lens [12], logic elements [13], nondestructive evaluation [14] and energy-harvesting devices [15]. Recently, we have explored the possibility of nanoscale counterpart of nonlinear granular crystals, finding it promising for shock mitigation and signal processing [16–20]. We have shown that nanoscale homogeneous carbon nanotube lattice exhibits extraordinary attenuation performance upon high-velocity impact. In addition, its nonplastic energy dissipation mechanism makes it advantageous over traditional energy dissipation structures for being repeatable and reusable [17]. The effectiveness and repeatability actually result from the dissipative and flexible nature of carbon nanotubes [21,22]. A disadvantage of this system is that upon relatively low impact velocities (<1000 m/s), the attenuation performance is not ideal because the external energy input is not high enough for carbon nanotube lattice to dissipate effectively [17]. Thus, impact in this velocity domain can still cause severe damages. Inspired by well-established macroscopic granular dimer chain [11,23–25], we introduce mass mismatch to construct a one-dimensional (1D) single-walled carbon nanotube (SWNT) dimer lattice, characterized by only one nondimensional parameter, the mass ratio. Through molecular dynamics (MD) simulation, we find that inherent resonance occurs for certain mass ratio, leading to significant stress wave attenuation. The joint effect of mass mismatch-induced resonance and dissipative nature of carbon nanotube lattice makes it ideal upon both high and low impact velocities. Furthermore, the lightweight of the dimer lattice improves the specific energy absorption (*SEA*) to a great extent.

## 2. Molecular dynamic simulation

The descriptions of 1D SWNT dimer lattice are provided as

* Corresponding author. Department of Automotive Engineering, School of Transportation Science and Engineering, Beihang University, Beijing, 100191, China.
*E-mail address:* junxu@buaa.edu.cn (J. Xu).

http://dx.doi.org/10.1016/j.carbon.2017.02.009
0008-6223/

below. The lattice is composed of 35 SWNTs, aligned parallelly. The symmetry plane normal to central axis of each SWNT coincides. The distance between the geometrical centers of adjacent SWNTs satisfies equilibrium requirement, guaranteeing a zero pre-compression of the lattice. The equilibrium spacing of SWNTs with various sizes can be found in Ref. [26]. Details of MD simulation are provided in Appendix 1. The first SWNT is rendered with an initial velocity $v_{imp}$, serving as the stress wave generator. Impact velocity is set as $v_{imp} = 400$ m/s, a relatively low velocity at nanoscale. Stress wave attenuation is indicated by transmission rate $\eta$, defined as the ratio of the maximum particle velocities of the last SWNT and the first SWNT, i.e. $\eta = v_{rec}/v_{imp}$. Mass ratio is denoted as $\beta$ $(0 < \beta \leq 1)$. To create mass mismatch, two strategies are considered in this work. One is varying SWNTs' length with the diameter fixed and the other way is varying the diameter with the length fixed, as are illustrated in Fig. 1. These two mass mismatch configurations are referred to as a *length-mismatch* dimer and a *diameter-mismatch* dimer respectively. For both strategies, the diameters of SWNTs are larger than the lengths such that the effect of wave propagation perpendicular to the direction of 1D alignment is minimized, making make the problem closer to a quasi-1D one. Simulation results based on two configurations for homogeneous lattice ($\beta = 1$) and dimer lattice ($\beta = 0.5$) are summarized in Table 1 and Table 2. One may easily conclude that upon $v_{imp} = 400$ m/s, 1D homogeneous SWNT lattices with all lengths and diameters studied support non-dissipative stress wave. For *length-mismatch* dimers, transmission rates are length-independent, suggesting that the dynamics of the system is only determined by mass ratio. A great advantage of this mismatch configuration is that for various mass ratios, the diameters of all components are identical, which successfully prevents the occurrence of nanoscale contact problem. For *diameter-mismatch* dimers, due to the homogeneity in components' length, mass ratio equals to diameter ratio. According to the results in the last three rows in Table 2, for a fixed diameter ratio, transmission rate varies with the absolute value of the diameter and no clear tendency is observed. This uncertainty may result from the introduction of contact heterogeneity. To pursue a robust system output with respect to mass ratio, the following study is based on the *length-mismatch* dimer.

**Table 1**
MD simulation results of 1D homogeneous SWNT lattice ($\beta = 1$) upon $v_{imp} = 400$ m/s for various lengths and diameters of SWNTs.

| SWNT | | Transmission rate $\eta$ |
|---|---|---|
| Length (Å) | Diameter (Å) | |
| 3.692 | 13.570 | 97.3% |
| 6.153 | 13.570 | 97.0% |
| 8.614 | 13.570 | 97.5% |
| 11.076 | 13.570 | 96.4% |
| 6.153 | 18.998 | 96.5% |
| 6.153 | 27.140 | 93.5% |

**Table 2**
MD simulation results of 1D dimer SWNT lattice with $\beta = 0.5$ upon $v_{imp} = 400$ m/s for various lengths and diameters of SWNTs.

| Heavy SWNT | | Light SWNT | | Transmission rate $\eta$ |
|---|---|---|---|---|
| Length (Å) | Diameter (Å) | Length (Å) | Diameter (Å) | |
| 6.153 | 13.570 | 2.461 | 13.570 | 80.5% |
| 8.614 | 13.570 | 3.692 | 13.570 | 80.2% |
| 11.076 | 13.570 | 4.923 | 13.570 | 79.5% |
| 7.384 | 27.319 | 7.384 | 13.570 | 75.1% |
| 7.384 | 32.567 | 7.384 | 16.283 | 66.3% |
| 7.384 | 37.995 | 7.384 | 18.997 | 78.8% |

## 3. Theoretical modeling

The mass ratio-governed stress wave attenuation of SWNT dimer lattices is a relatively counterintuitive phenomenon, namely nonlinear resonance. It has been reported that in 1D granular dimer chains at macroscale, for an infinite number of mass ratios, inherent nonlinear resonances or anti-resonances could happen, resulting in a maximum amplification and complete elimination of oscillating wave tails respectively [27]. For resonances, propagating pulse is

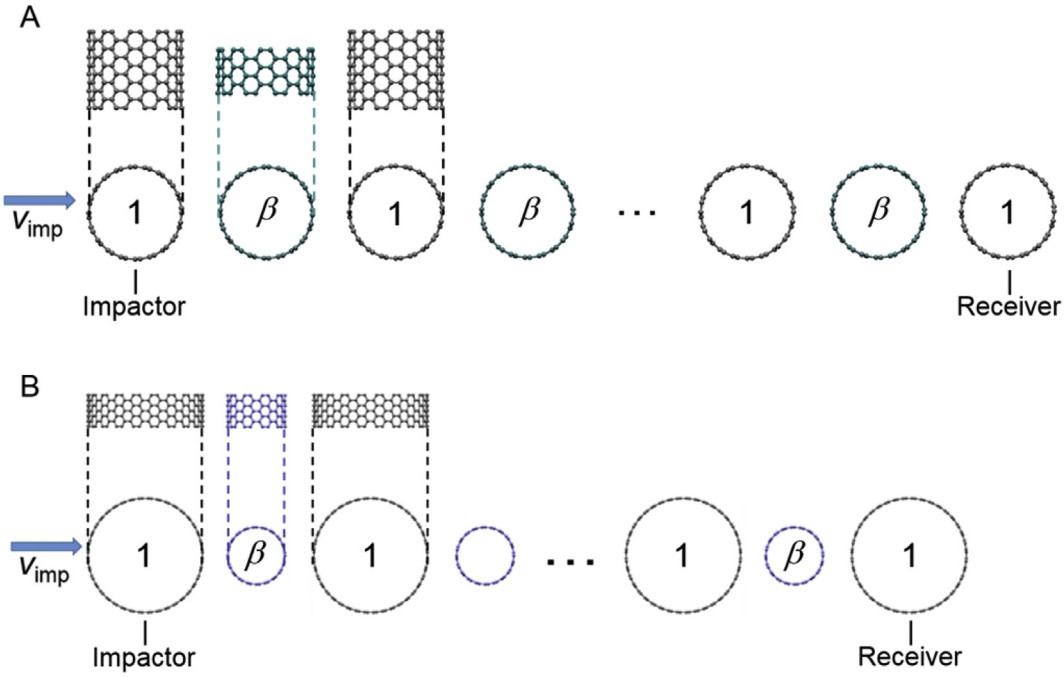


**Fig. 1.** The schematic of the 1D SWNT dimer lattices. (A) a *length-mismatch* dimer; (B) a *diameter-mismatch* dimer. (A colour version of this figure can be viewed online.)

significantly attenuated because under this circumstance, the radiated energy to the far field is a maximum. Mass ratios for resonance are determined by the integral relations between the characteristic frequencies of two phases of motion of the light grains, i.e. the squeeze mode and the collision mode. The squeeze mode happens during the arrival of the propagating pulse, when the light grain is continuously compressed by adjacent heavy grains. The collision mode happens after the primary pulse has propagated through the light grain where heavy and light grains collide with each other [24]. When the two characteristic frequencies are equal, i.e. a 1:1 resonance occurs, leading to the strongest attenuation. Theoretically, this resonance phenomenon is fully re-scalable with respect to impact velocity, i.e. the predicted transmission rate can be realized for arbitrarily input wave amplitudes. In this work, we apply this concept to model the stress wave attenuation at nanoscale.

Due to the strong nonlinearity and high complexity of the intermolecular van der Waals force, the interactions between adjacent SWNTs are accounted for by a nonlinear spring model $F = k\delta^n$ as a powerful and successful simplification [16], where $F$ is interaction force; $\delta$ is the overlapping distance of van der Waals radii; $k$ is stiffness constant and $n$ is nonlinear index. Upon relatively low impact velocities ($v_{\mathrm{imp}} < 500$ m/s), the stress wave attenuation due to SWNT's dissipation nature is trivial. Then the governing equations of motion can be given as

$$\begin{aligned} &m_i\frac{\mathrm{d}^2u_i}{\mathrm{d}t^2} = k\left[(u_{i-1}-u_i)_+^n - (u_i-u_{i+1})_+^n\right] \\ &m_{i+1} = \beta m_i \\ &m_{i+1}\frac{\mathrm{d}^2u_{i+1}}{\mathrm{d}t^2} = k\left[(u_i-u_{i+1})_+^n - (u_{i+1}-u_{i+2})_+^n\right] \\ &i = 1,\ 3,\ 5,\ldots \end{aligned} \tag{1}$$

where $u_i$ is the displacement of $i$th SWNT. The subscript $(+)$ is defined by $[r]_+ = \max(0, r)$. Normalization is introduced as

$$\begin{aligned} &x_i = k_n^{\frac{1}{n}}u_i \\ &\tau = \left(\frac{k_n^{\frac{1}{n}}}{m}\right)^{\frac{1}{2}}t \end{aligned} \tag{2}$$

To this end, we obtain the governing equations with only one nondimensional parameter mass ratio $\beta$ as

$$\begin{aligned} &\frac{\mathrm{d}^2x_i}{\mathrm{d}\tau^2} = (x_{i-1}-x_i)_+^n - (x_i-x_{i+1})_+^n \\ &\beta\frac{\mathrm{d}^2x_{i+1}}{\mathrm{d}\tau^2} = (x_i-x_{i+1})_+^n - (x_{i+1}-x_{i+2})_+^n \\ &i = 1,\ 3,\ 5,\ldots \end{aligned} \tag{3}$$

Eq. (3) is re-scalable with respect to impact velocity in the low-velocity domain, because upon higher impact velocities, a dissipative term should be included due to the dissipative nature of SWNT.

## 4. Results and discussions

In this section, the focus is on the transmission rate $\eta$ as a function of mass ratio $\beta$ and the resonance zone (RZ) on $\beta$ axis. Setting $n = 1.5$, consistent with previous studies based on Hertzian contact [24], the calculation based on governing Eq. (3) is compared to the results of MD simulations of in Fig. 2, where (10,10), (14,14), (20,20), (24,24), (26,26), (30,30) length-mismatch dimers are involved. The diameters are 13.570 Å, 18.998 Å, 27.140 Å, 32.567 Å, 35.281 Å, 40.709 Å respectively.

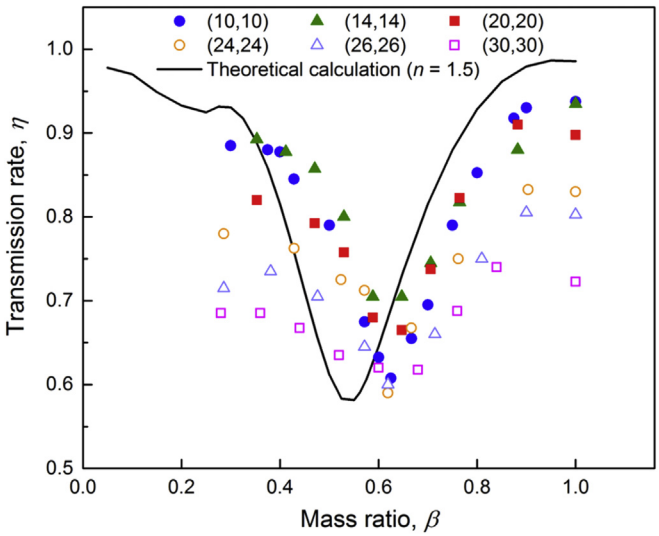


**Fig. 2.** Comparison between the results of MD simulations and theoretical calculations of various *length-mismatch* dimers when $n = 1.5$. (A colour version of this figure can be viewed online.)

For all the MD simulation results in Fig. 2, a strong 1:1 resonance is achieved at $\beta \approx 0.60$. This indicates that the mass ratio for 1:1 resonance is independent of the diameter of SWNT. The trends of theoretically calculated curve and simulation results of (10,10), (14,14), (20,20) SWNT lattices are in a good agreement. However, for SWNTs with larger diameters, the results tend to be "flattened out". This is because the total transmission is a superposition of intrinsic resonance and dissipation of SWNTs, and larger SWNT has greater dissipation effect. When the diameter reaches ~40 Å, the phenomenon of transmission valley becomes insignificant and dissipation of SWNTs plays a more important role. Therefore, different from macroscopic granular dimer chains, SWNT dimer lattices are not fully re-scalable with respect to impact velocity due

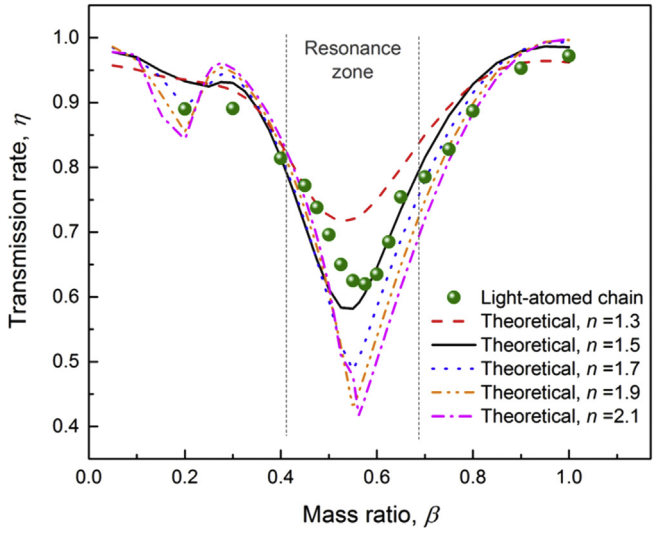


**Fig. 3.** Comparison between MD simulation result of the *light-atomed* dimer and theoretical calculations for various nonlinear indices $n$. (A colour version of this figure can be viewed online.)

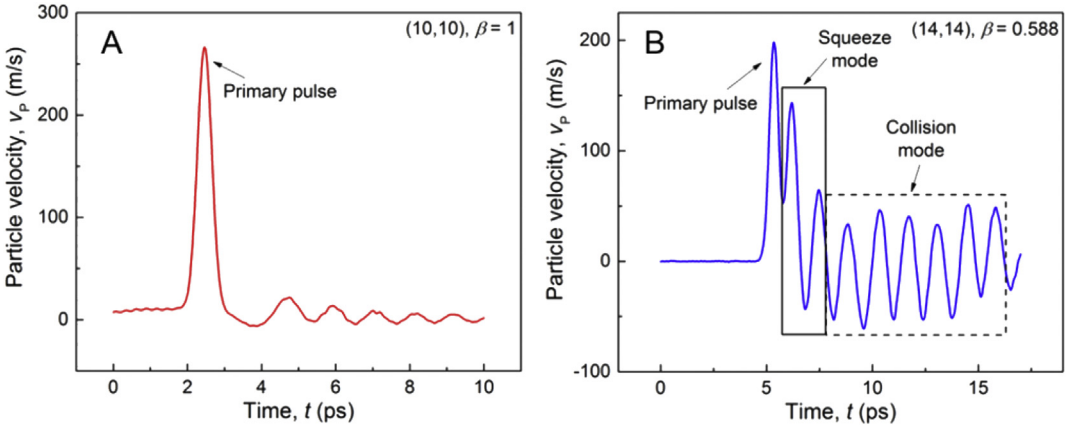


**Fig. 4.** Comparison between the wave shapes of (A) 1D homogeneous (10,10) SWNT lattice and (B) (14,14) SWNT dimer lattice with $\beta = 0.588$. In the dimer lattice, the wave shape of a light SWNT is extracted. (A colour version of this figure can be viewed online.)

**Table 3**
Summary of resonant frequencies.

| Type of SWNT | Mass ratio, $\beta$ | Resonance frequency of squeeze mode, $f_s$ (THz) | Resonance frequency of collision mode, $f_c$ (THz) |
|---|---|---|---|
| (10,10) | 0.60 | 806 ± 5 | 800 ± 20 |
| (14,14) | 0.588 | 690 ± 4 | 667 ± 16 |

to the dissipative nature of SWNTs. In addition, it is shown that further increasing the diameter will not shift the resonance zone. Therefore, to achieve a broader range of wave tuning and system output, SWNTs smaller than (20,20) are suggested. Note that there exists a slight inconsistency between simulation and theoretical results in terms of the position of RZ on $\beta$ axis. The reason could be revealed by constructing an imaginary *light-atomed* dimer whose components have the same geometry but various masses to achieve the mass mismatch to eliminate geometric heterogeneity. Here, the components are chosen as (10,10) SWNT with an axial length of $l = 6.153$ Å. The MD simulation result upon $v_{imp} = 400$ m/s and theoretical calculations for various nonlinear indices $n = 1.3, 1.5, 1.7, 1.9, 2.1$ are compared in Fig. 3 since no explicit analytical expression is available.

Fig. 3 shows a good consistency between the simulation result of *light-atomed* dimer and theoretical calculations, suggesting that the inconsistency of RZ in Fig. 2 actually results from the geometric difference of the components in the *length-mismatch* dimer. Although the difference in length may result in various contact stiffness, we are able to show theoretically that in the absence of dissipation, the transmission rate is independent of contact stiffness (see Appendix 2). Compared to theoretical results, the *length-mismatch* dimer translates RZ towards larger values of $\beta$, while the size of RZ remains unaltered. In addition, it is observed in Fig. 3 that higher nonlinear index $n$ leads to better resonance-induced attenuation but converges to ~0.4, while the position of RZ remains almost unaffected. Therefore, we are inspired by above observations that for the optimal design of attenuative dimer lattices, apart from a mass ratio in the center of RZ, the interaction nonlinearity of neighboring particles should be high but the nonlinear index is not necessarily higher than 2. In Eq. (3), mass ratio $\beta$ near the RZ is not a small parameter (which requires

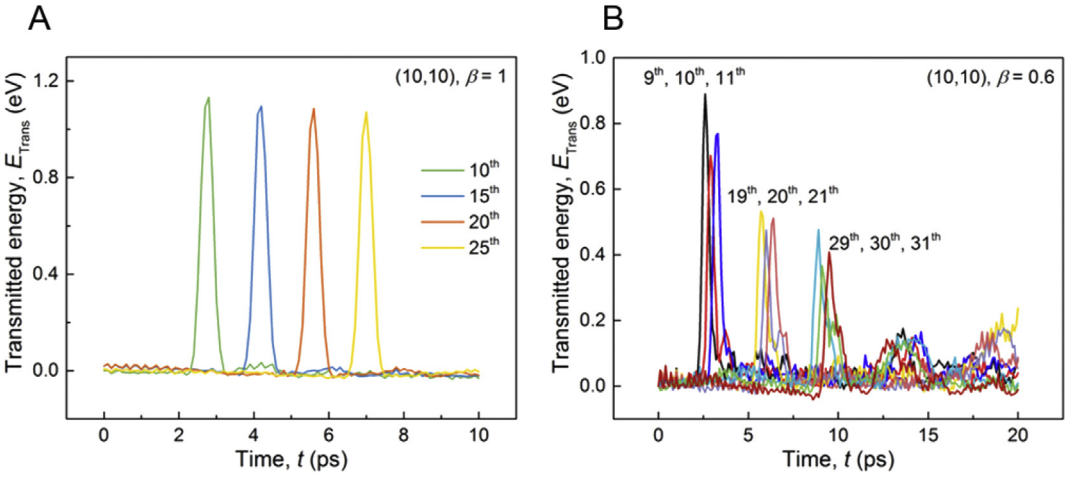


**Fig. 5.** Transmitted energy histories of (A) 1D homogeneous (10,10) SWNT lattice and (B) (10,10) SWNT dimer lattice with $\beta = 0.6$. (A colour version of this figure can be viewed online.)

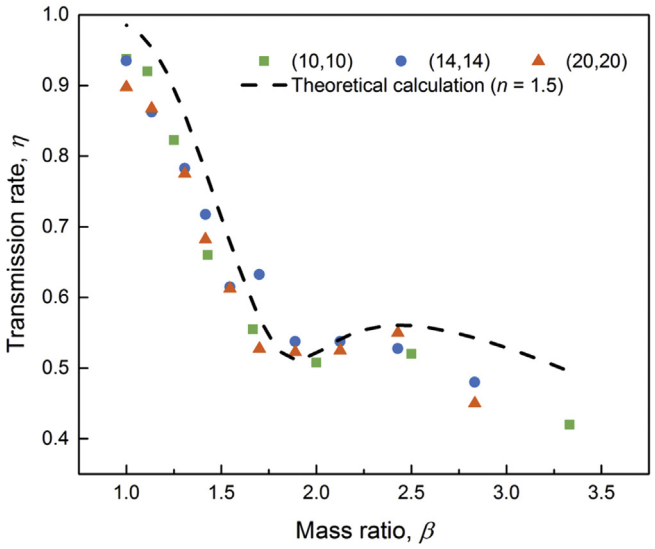


**Fig. 6.** Comparison between the results of MD simulation and theoretical calculation for SWNT dimer lattices with ($\beta > 1$). (A colour version of this figure can be viewed online.)

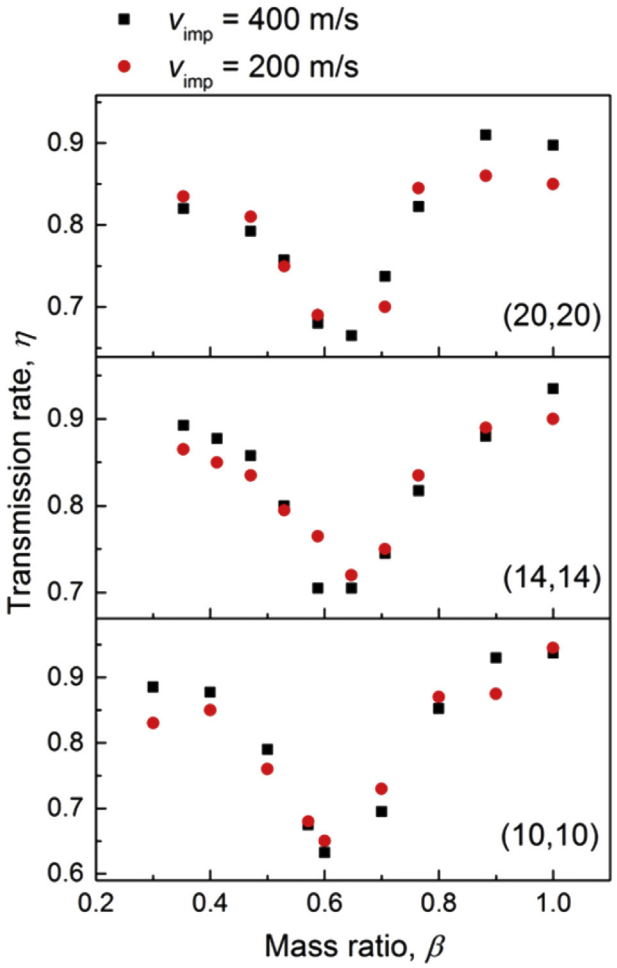


**Fig. 7.** Comparison of transmission rates of SWNT dimer lattices upon $v_{imp} = 400$ m/s and $v_{imp} = 200$ m/s of various types of SWNT. (A colour version of this figure can be viewed online.)

$0 < \beta \ll 1$). It is not possible to perform asymptotic analysis, whose accuracy is validated only in the limit of small $\beta$ [25]. We can only determine the position of RZ by numerically solving Eq. (3).

We extract the particle velocity-time histories of heavy and light SWNTs to check whether the wave behaviors are consistent with the theoretical descriptions of nonlinear resonance discussed earlier. As can be seen in Fig. 4, oscillating tails are small in homogeneous (10,10) SWNT lattice ($\beta = 1$) and large in strongly resonant (14,14) SWNT dimer ($\beta = 0.588$). The squeeze mode and the collision mode with equal characteristic frequencies can be clearly observed in Fig. 4(B), corresponding to 1:1 resonance. These observations further confirm us that in SWNT dimer lattices, strong attenuation rises from the amplification of the oscillating tails of propagating pulse. The resonant frequencies of (10,10) and (14,14) SWNT dimer lattices are summarized in Table 3, where the resonance frequencies of squeeze mode $f_s$ and collision mode $f_c$ are equal.

Energy distribution in SWNT lattices is studied in Fig. 5, where transmitted energy of certain SWNTs are extracted. In the homogeneous (10,10) SWNT lattice (Fig. 5(A)), the transmitted energy has little dissipation as the stress wave propagates and the tails are insignificant. This suggests that homogeneous SWNT lattice transmits energy efficiently within the impact velocity domain studied here. However, in the (10,10) SWNT dimer lattice with $\beta = 0.6$ (Fig. 5(B)), the transmitted energy has a large dissipation, together with significant tails where the dissipated energy goes. It is also observed that light SWNTs (10th, 20th and 30th SWNTs in Fig. 5(B)) transmit less energy than adjacent heavy ones.

For the completeness of study, results of MD simulation and theoretical calculation are compared for SWNT dimer lattices with $\beta > 1$ in Fig. 6 and a good consistency is observed for various types of SWNT. The transmission rates upon $v_{imp} = 400$ m/s and $v_{imp} = 200$ m/s of various types of SWNT are compared in Fig. 7. As is shown, the system response has a similar pattern if the impact velocity further decreases.

Now, the stress wave attenuation and energy absorption ability of strongly-resonant SWNT dimers ($\beta = 0.6$) is evaluated in comparison to homogeneous SWNT lattices, where (10,10), (14,14) and (20,20) SWNT lattices are tested. The performances of the two configurations are compared in Fig. 8. Greatly enhanced attenuation upon relatively low impact velocities ($v_{imp} < 1000$ m/s) is observed. For higher impact velocities, attenuation enhancements become less effective. Because in this impact velocity domain, the attenuation of the dissipative nature is a dominant factor. For SWNTs with smaller diameters, enhancement of attenuation is greater, because they are relatively less dissipative compared with larger SWNTs, thus the effect of resonance is more evident. Furthermore, compared with homogeneous lattice, the strongly-resonant dimer lattice is 22% lighter while having a better attenuation performance upon all impact velocities investigated. Thus, the mechanism of mass mismatch-induced resonance can achieve an enhancement (>30%) of *SEA* upon high-velocity impact. Therefore, the introduction of mass mismatch to 1D SWNT lattice can achieve an overall enhancement of stress wave attenuation and energy absorption ability. The dissipation mechanism of nanoscale SWNT dimer lattice addressed in this work is fundamentally different from macroscale cellular systems, which is accounted for by the effect of inertial stabilization, shock wave and strain rate hardening etc [28,29].

## 5. Concluding remarks

In summary, a 1D SWNT dimer lattice is constructed to overcome the ineffectiveness of 1D homogeneous SWNT lattice upon

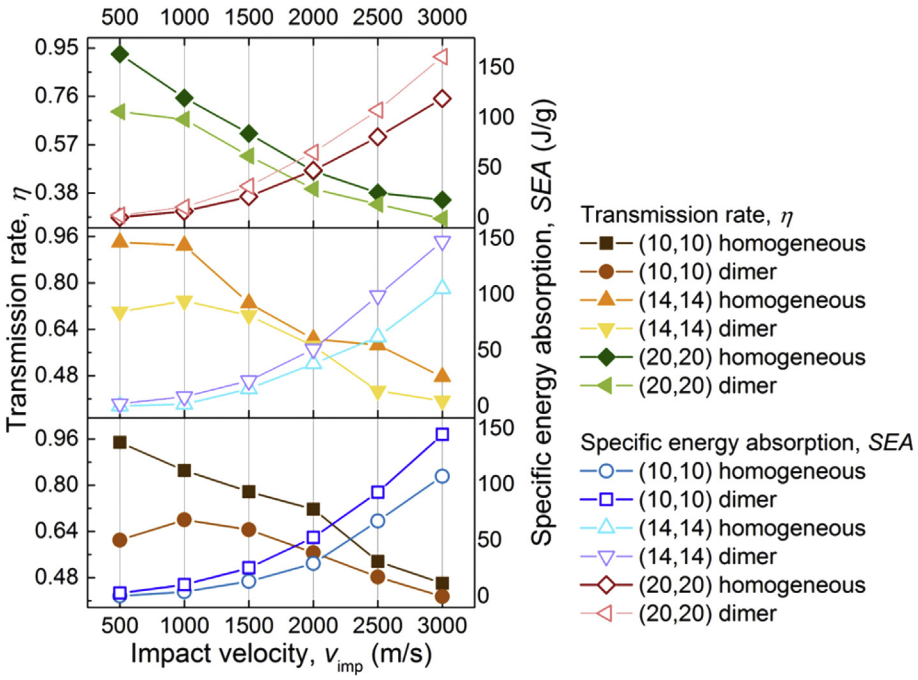


**Fig. 8.** Comparison between attenuation performance and *SEA* of 1D homogeneous SWNT lattice ($\beta = 1$) and SWNT dimer ($\beta = 0.6$). (A colour version of this figure can be viewed online.)

relatively low impact velocities ($v_{imp} < 1000$ m/s). Under specific mass ratio, a strong inherent resonance happens, resulting in an evident attenuation of the propagating pulse. The joint effect of mass mismatch-induced resonance and dissipative nature of carbon nanotube lattice make it ideal for both high and low-velocity impacts. Because enhanced attenuation performance and lightweight are simultaneously achieved by creating mass mismatch, *SEA* of the SWNT lattice is significantly improved. This work suggests a strategy of efficient stress wave attenuation and energy absorption via manipulating the inherent dynamics of the periodic structured system and shed light on the novel design of carbon based nanoscale wave tuning devices using nonlinear granular phononic crystals.

## Acknowledgements

This work is financially supported by start-up funds of "The Recruitment Program of Global Experts" awardee from Beihang University (YWF-16-RSC-011).

## Appendix A. Supplementary data

Supplementary data related to this article can be found at http://dx.doi.org/10.1016/j.carbon.2017.02.009.

## References

[1] R. Martinezsala, J. Sancho, J. Sánchez, V. Gómez, J. Llinares, F. Meseguer, Sound-attenuation by sculpture, Nature 378 (6554) (1995) 241, 241.
[2] M. Sigalas, E. Economou, Elastic and acoustic wave band structure, J. Sound. Vib. 158 (2) (1992) 377–382.
[3] M.S. Kushwaha, P. Halevi, L. Dobrzynski, B. Djafari-Rouhani, Acoustic band structure of periodic elastic composites, Phys. Rev. Lett. 71 (13) (1993) 2022–2025.
[4] Z. Liu, X. Zhang, Y. Mao, Y.Y. Zhu, Z. Yang, C.T. Chan, P. Sheng, Locally resonant sonic materials, Science 289 (5485) (2000) 1734–1736.
[5] S.A. Cummer, J. Christensen, A. Alù, Controlling sound with acoustic metamaterials, Nat. Rev. Mater. 1 (2016) 16001.
[6] K.L. Johnson, Contact Mechanics, Cambridge University Press, Cambridge [Cambridgeshire]; New York, 1987.
[7] V.F. Nesterenko, Propagation of nonlinear compression pulses in granular media, J. Appl. Mech. Tech. Phys. 24 (5) (1983) 733–743.
[8] A. Lazaridi, V. Nesterenko, Observation of a new type of solitary waves in a one-dimensional granular medium, J. Appl. Mech. Tech. Phys. 26 (3) (1985) 405–408.
[9] C. Coste, E. Falcon, S. Fauve, Solitary waves in a chain of beads under Hertz contact, Phys. Rev. E 56 (5) (1997) 6104–6117.
[10] V.F. Nesterenko, Dynamics of Heterogeneous Materials, Springer, New York, 2001.
[11] N. Boechler, G. Theocharis, S. Job, P.G. Kevrekidis, M.A. Porter, C. Daraio, Discrete breathers in one-dimensional diatomic granular crystals, Phys. Rev. Lett. 104 (24) (2010) 244302.
[12] A. Spadoni, C. Daraio, Generation and control of sound bullets with a nonlinear acoustic lens, Proc. Natl. Acad. Sci. U. S. A. 107 (16) (2010) 7230–7234.
[13] F. Li, P. Anzel, J. Yang, P.G. Kevrekidis, C. Daraio, Granular acoustic switches and logic elements, Nat. Commun. 5 (2014) 5311.
[14] J. Yang, C. Silvestro, S.N. Sangiorgio, S.L. Borkowski, E. Ebramzadeh, L.D. Nardo, C. Daraio, Nondestructive evaluation of orthopaedic implant stability in THA using highly nonlinear solitary waves, Smart Mater. Struct. 21 (1) (2012) 012002.
[15] L.-Y. Wu, L.-W. Chen, C.-M. Liu, Acoustic energy harvesting using resonant cavity of a sonic crystal, Appl. Phys. Lett. 95 (1) (2009) 013506.
[16] J. Xu, B. Zheng, Y. Liu, Solitary wave in one-dimensional buckyball system at nanoscale, Sci. Rep. 6 (2016) 21052.
[17] J. Xu, B. Zheng, Highly effective energy dissipation system based on one-dimensionally arrayed short single-walled carbon nanotubes, Extreme Mech. Lett. 9P2 (2016) 336–341.
[18] J. Xu, B. Zheng, Quantitative tuning nanoscale solitary waves, Carbon 111 (2017) 62–66.
[19] J. Xu, B. Zheng, Stress wave propagation in two-dimensional buckyball lattice, Sci. Rep. 6 (2016) 37692.
[20] B. Zheng, J. Xu, Mechanical Wave Propagation within Nanogold Granular Crystals, Phys. Rev. Appl. (in submission).
[21] S. Iijima, Helical microtubules of graphitic carbon, Nature 354 (6348) (1991) 56–58.
[22] M.-F. Yu, O. Lourie, M.J. Dyer, K. Moloni, T.F. Kelly, R.S. Ruoff, Strength and breaking mechanism of multiwalled carbon nanotubes under tensile load, Science 287 (5453) (2000) 637–640.
[23] E.B. Herbold, J. Kim, V.F. Nesterenko, S.Y. Wang, C. Daraio, Pulse propagation in a linear and nonlinear diatomic periodic chain: effects of acoustic frequency band-gap, Acta Mech. 205 (1) (2009) 85–103.
[24] K.R. Jayaprakash, Y. Starosvetsky, A.F. Vakakis, New family of solitary waves in granular dimer chains with no precompression, Phys. Rev. E 83 (3) (2011) 036606.
[25] K.R. Jayaprakash, Y. Starosvetsky, A.F. Vakakis, O.V. Gendelman, Nonlinear

resonances leading to strong pulse attenuation in granular dimer chains, J. Nonlinear Sci. 23 (3) (2013) 363–392.
[26] L.A. Girifalco, M. Hodak, R.S. Lee, Carbon nanotubes, buckyballs, ropes, and a universal graphitic potential, Phys. Rev. B 62 (19) (2000) 13104–13110.
[27] K.R. Jayaprakash, A.F. Vakakis, Y. Starosvetsky, Strongly nonlinear traveling waves in granular dimer chains, Mech. Syst. Signal Proc. 39 (1–2) (2013) 91–107.
[28] Y. Liu, T.A. Schaedler, X. Chen, Dynamic energy absorption characteristics of hollow microlattice structures, Mech. Mater. 77 (2014) 1–13.
[29] Y. Liu, T.A. Schaedler, A.J. Jacobsen, X. Chen, Quasi-static energy absorption of hollow microlattice structures, Compos. B Eng. 67 (2014) 39–49.